Indian Journal of Engineering & Materials Sciences
Vol. 27, April 2020, pp. 267-276

Study of surface integrity and effect of process parameters in wire electrical discharge turning of Ti-6Al-4V

Akash Nag[a], Ashish Kumar Srivastava[b*], Amit Rai Dixit[a], Amitava Mandal[a], Alok Kumar Das[a]

[a]Indian Institute of Technology (I.S.M) – Dhanbad 826004, Jharkhand, India

[b]G L Bajaj Institute of Technology and Management, Greater Noida, Gautam Budha Nagar 201306, India

Received: 27 November 2017; Accepted: 08 January 2019

Wire electrical discharge turning set-up has been developed by modifying the conventional five axes CNC WEDM machine. The main objective of this setup is to achieve cylindrical forms on hard to cut materials. This work focuses on the study of effect of input process parameters like pulse on-time, pulse off time, gap voltage, spindle rotational speed on output responses like surface roughness, material removal rate and wire wear ratio. A mathematical model of responses has been developed using response surface methodology and the optimal value of process parameters has been obtained by desirability function. Surface morphology studies of the machined surface and the worn-out wire has also been elaborated by FE-SEM images. The results show that with an increase in machining parameters value except pulse-on time, all the desired machining outcome decreases. Surface roughness, material removal rate and wire wear ratio have been found in the range of 1.99 µm – 1.37 µm, 7.55 – 13.66 mm^3/min and 0.05–0.08, respectively. The formation of thick recast layer over the machined surface has also been discussed. The reduction in wire dimension has been calculated by optical microscopy and its morphology has been discussed by FE-SEM images.

Keywords: Surface integrity, Wire wear, Wire electrical discharge turning, Ti6Al4V

1 Introduction

With the increasing demand and application of advance materials like Titanium alloys, Hastelloy, Nimonic and Inconel, newer advance machining methods are being developed rapidly. Titanium alloy namely Ti6Al4V is being used in various domains, primarily in aerospace industry and biomedical implants. It is due to its high strength to weight ratio and property such as corrosion resistant. Machining of Ti6Al4V is not similar to other conventional material due to its chemical affinity with conventional cutting tools which causes chemical wear and formation of build-up edges[1]. Among various non-traditional processes, wire electrical discharge machining (WEDM) is largely used for machining of difficult to machine materials[2]. WEDM thermally erode the workpiece material by generating electrical discharges between the wire and the workpiece material, in presence of dielectric fluid[3]. These electrical discharges produced, causes melting and vaporising of the material, leading to its erosion in form of craters[4]. This process is largely used to manufacture intricate three-dimensional and two-dimensional shapes from electrically conductive material[5]. The material strength and hardness does not affect the process and affect the tool wear[6]. WEDM process has low cutting force, which makes it suitable to machine delicate components and make intricate engineering shapes on hard to cut material with better surface finish[7]. Wire electrical discharge turning (WEDT) is a process in which a rotary motion is given to the workpiece to be turned. An external setup for imparting this motion to the work material is attached to the conventional CNC WEDM machine, for machining cylindrical forms[8]. Figure 1 shows the schematic diagram of the WEDT process. Electrical discharges originate between the rotating workpiece and the wire. This discharges from the wire jump to the workpiece material through insulating fluid, which erodes the surface by melting and vaporising. This phenomenon takes place due to the heat developed by the sparks where the temperature reaches nearly 7,000 °C to 11,000 °C[9, 10]. These molten particles are flushed out of the workpiece material with the flow of de-ionized water.

Many research papers are available in the WEDM domain, however very limited work has been reported for WEDT. Masuzawa *et al.*[11] were first to use

*Corresponding author (E-mail: ashish7185@gmail.com)

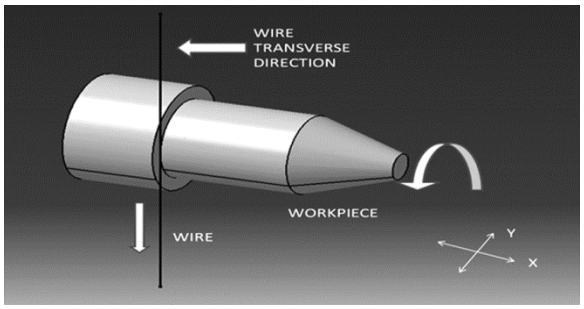

Fig. 1 — Concept wire electrical discharge turning.

WEDM to machine cylindrical parts. Shafts and micro pins were fabricated for micro electrical discharge machining operations. Qu *et al.*[12] investigated cylindrical wire electrical discharge machining (CWEDM) using carbide and brass work material to investigate the influence of input parameters on material removal rate (MRR), surface roughness (SR) and roundness. They concluded that higher MRR was obtained for CWEDM than conventional WEDM and SR was significantly influenced by pulse on time and feed rate. Mohammadi *et al.*[13] studied the influence of input parameters on SR and roundness of cemented steel. The experimental result showed that power had a significant effect on SR. Regression analysis was used to generate mathematical model to optimise the machining parameters. Haddad *et al.*[14–16] investigated WEDT on AISI D3 tool steel. They found that voltage and power had a direct impact on MRR and SR whereas spindle rotation and pulse off time had an inverse effect on them. Moreover, for roundness, spindle speed and pulse off time were significant factors. Janardhan and Samuel[17] analysed the WEDT by using pulse discrimination algorithm. They observed that MRR, SR and roundness varied inversely with decreasing spark gap and pulse off time whereas rotational speed and servo feed had a direct effect on the output responses. Experimental runs were conducted by Gjeldum *et al.*[18] to generate a mathematical model for MRR using pulse duration, pulse current and rotational speed on X5CrNil8-10 steel. It was reported that pulse current significantly influenced MRR. Artificial neural network technique yielded better results as compared to the full factorial method in regression analysis. Weingartner *et al.*[19, 20] developed a model to analyse the response of rotational speed on generated surface craters. The study revealed that arc column drifts over the workpiece easily at higher rotational speed operation which results into the increase in craters, along that direction. Rajkumar *et al.*[21] used response surface methodology (RSM) technique to observe the effect of input parameters such as pulse-on time, gap voltage and spindle speed on SR and MRR using Al/SiCp metal matrix composite as work material. Giridharan and Samuel[22] studied the influence of machining parameters on SR and MRR along with energy consumption on AISI 4340. The results showed that keeping spindle rotation and servo feed constant, energy consumption decreased with an increase in pulse-off time. Garg *et al.*[23] investigated WEDM of Ti-6Al-4V and analysed the effect of machining parameters on cutting speed and roughness. Zhu *et al.*[24] fabricated micro rotary parts with a larger aspect ratio. The results showed that with low radial infeed, high MRR was achieved. Kanthababu *et al.*[25] investigated MRR and SR of Al/SiCp based MMC. Influence of different reinforcement particle sizes was also studied. They observed that material with lower particle size led to greater SR and lesser MRR as compared to material with larger particle size.

Very few articles related to the analysis of surface integrity of machined surface generated after WEDT operation and wire electrode were found in the open literature. In the present study, WEDT operation is performed on Ti6Al4V work material. The effect of technological parameters like pulse on time, pulse off time, gap voltage and spindle speed on output responses such as SR, MRR and wire wear ratio (WWR) are analysed. Mathematical model of the responses are developed and optimised using RSM and desirability function approach, respectively. Surface topographical images were captured by field emission scanning electron microscopy (FE-SEM) to study the surface generated by the process and also to analyse the surface defects induced due to the thermal effect of the process.

2 Materials and Methods

In this study, turning operation is performed on in-house fabricated turning attachment which was retrofitted to the existing 5-axes Elektra Maxicut 734 CNC WEDM machine. The purpose of the turning setup is used to provide an additional degree of freedom in the rotational direction. The wire is moved in traverse direction against the cylindrical surface of the workpiece to perform the machining. DC motor with a variable frequency drive device is used for varying rotational speeds and by using a conductive assembly, the workpiece is given a positive potential whereas the wire is connected to the negative

potential to achieve high erosion rate of the workpiece[26]. The experimental setup is presented in Fig. 2. The rotary setup comprises of DC motor, rotating spindle, microprocessor-based controller, proximity sensor, belt and pulley drive.

Ti6Al4V cylindrical rod of 8 mm diameter and 30 mm long is used for the experiments. Titanium alloys due to its low specific heat and thermal conductivity result in high machining temperature. Moreover, it maintains its mechanical property at elevated temperature and undergoes work hardening which leads to high machining forces[27, 28]. The composition of Ti6Al4V is presented in Table 1. Wire electrode of 0.25mm diameter, made of zinc coated brass is used for experiments.

RSM with central composite design is used to design the experiment. RSM is a statistical technique that is useful to analyse a problem in which the output responses depend on more than one input variables and the main goal is to optimise these output responses[29, 30]. Four technologicalfactors namely pulse on time, pulse off time, gap voltage and spindle speed are considered from literature review and three different levels of each parameter are selected. The range of the technological factors were selected from pilot experiments. Wire breakage was observed while machining beyond these range of parameters (Table 2). The constant parameters and their values are shown in Table 3.

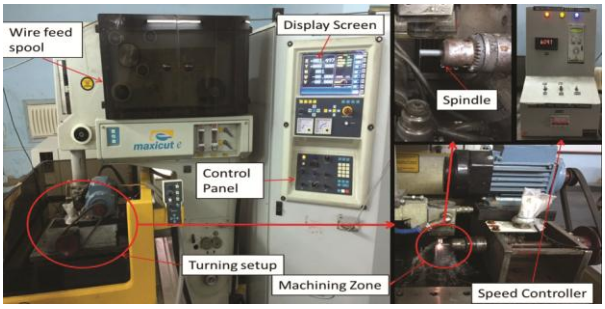

Fig. 2 — Experimental setup for WEDT.

Table 1 — Elemental constitution of Ti-6Al-4V.

Elements	Titanium (Ti)	Aluminium (Al)	Vanadium (V)
Percentage (%)	90	6	4

Table 2 — Process parameters and their levels.

Symbol	Parameters	Levels				
		1	2	3	4	5
A	Pulse on time (μs)	0.95	1.00	1.05	1.10	1.15
B	Pulse off time (μs)	170	180	190	200	210
C	Gap voltage (V)	20	30	40	50	60
D	Rotational speed (rpm)	200	300	400	500	600

In each experiment, a workpiece of 3mm length was turned, reducing the work piece diameter from 8mm to 5mm. SR was measured by mitutoyo make (SJ – 210) roughness tester. Four reading were taken from equally offset lines parallel to the axis of rotation. ISO 1997 standard was followed while taking measurements.The sampling length of 0.4 mm with cut-off value 2.5μmwas used. Mean values of these readings were taken for further analysis.

Machining time for every run was recorded and the MRR was calculated using Eq.(1).

$$MRR = \frac{\pi\times(D^2-d^2)\times l}{4\times t}(\text{mm}^3/\text{min}) \quad \ldots (1)$$

where, D, d, l and t are the initial diameter, final diameter, machining length and machining time respectively.

Due to spark generated during machining both the work material along with the wire also gets eroded which is called as wire wear[31]. WWR is the ratio of change in wire weight during machining to its original weight. The original wire weight for a unit time and wire weight after every experiment was measured. WWR was calculated using Eq. (2).

$$WWR = \frac{(w\times t)-W}{w\times t} \quad \ldots (2)$$

where, w is the original wire weight per unit time, W is the wire weight after machining and t is the machining time.

Regression analysis was performed using Minitab 17 statistical software for the experimental results (Table 4), to obtain an adequate model for the responses. The Analysis of variance test was performed to determinetechnological factors which significantly influence the output response (Table 5). Machined surface images were taken by FESEM machine to study the surface morphology of wire and machined surface.

3 Results and Discussion

Figure 3 shows Ti6Al4V work material before and after WEDT operation. 31 experiments were performed as per design of experiment. The

Table 3 — Constant process parameters.

Parameter	Value
Sensitivity	5
Wire feed (m/min)	1
Wire tension (KgF)	600
Deionized water conductivity(S) (mho)	13
Flow top (LPM)	6
Flow bottom (LPM)	6

Table 4 — Experimental table.

Run No	Ton(µs)	Toff(µs)	Gap Voltage(V)	RPM	Ra(µm)	MRR(mm^3/min)	WWR
1	1.10	180	30	300	1.999	13.66	0.0859
2	1.00	180	50	300	1.743	9.57	0.0647
3	1.05	190	40	400	1.689	9.91	0.0697
4	1.05	190	40	400	1.663	9.87	0.0697
5	1.00	200	30	300	1.638	10.68	0.0652
6	1.05	190	40	400	1.632	9.78	0.069
7	1.10	200	30	500	1.699	10.77	0.072
8	1.05	190	40	400	1.605	9.67	0.068
9	1.00	180	30	500	1.663	9.92	0.0723
10	1.05	190	40	400	1.634	9.56	0.068
11	1.05	170	40	400	1.827	10.73	0.0777
12	1.05	190	40	400	1.604	9.74	0.0691
13	1.05	190	40	600	1.46	8.55	0.0642
14	1.05	190	60	400	1.634	8.34	0.0586
15	1.05	190	20	400	1.843	11.87	0.0787
16	0.95	190	40	400	1.44	8.5	0.0593
17	1.05	210	40	400	1.454	9.06	0.058
18	1.10	200	50	500	1.553	8.94	0.0625
19	1.00	180	50	500	1.55	8.37	0.0605
20	1.05	190	40	200	1.822	11.751	0.0733
21	1.10	180	30	500	1.848	11.74	0.0804
22	1.10	180	50	300	1.923	11.65	0.074
23	1.05	190	40	400	1.68	9.79	0.0682
24	1.10	200	30	300	1.841	12.52	0.0765
25	1.10	200	50	300	1.755	10.79	0.0666
26	1.15	190	40	400	1.838	11.99	0.0792
27	1.00	200	30	500	1.439	9.2	0.0601
28	1.10	180	50	500	1.773	9.85	0.0695
29	1.00	180	30	300	1.823	11.52	0.0759
30	1.00	200	50	500	1.371	7.55	0.0508
31	1.00	200	50	300	1.503	8.89	0.0552

experimental Table and the obtained responses for each experiment are listed in Table 4.

Using the experimental data, analysis of variance (ANOVA) test was performed (Table 5). Model to be statistically significant, P-values of the model terms should be less than 0.05[32]. R-sq and R-Sq (Adj) for all the responses should tend to unity, which is needed for fitness of the model. The "lack of fit" values should be high which signifies whether the obtained model fit significantly for predicting the output responses within the specified experimental domain. Higher P-value of lack of fit and R-sq (pred) for all the output responses showed that the regression models formulated using the experimental values were highly significant and predictive to predict the output responses using the input parameter value within the selected domain.

Final regression equations for predicting the performance responses were obtained as follows.

$$SR = 2.284 + 2.047 \times Ton - 0.009454 \times Toff - 0.02709 \times Gap\,Voltage - 0.000855 \times RPM + 0.000276 \times Gap\,Voltage \times Gap\,Voltage \quad \ldots (3)$$

$$MRR = 100.9 - 111.0 \times Ton - 0.331 \times Toff - 0.1921 \times Gap\,Voltage + 0.00308 \times RPM + 65.3 \times Ton \times Ton + 0.000758 \times Toff \times Toff + 0.001283 \times Gap\,Voltage \times Gap\,Voltage + 0.000014 \times RPM \times RPM - 0.02125 \times Ton \times RPM \ldots (4)$$

$$WWR = 0.2569 - 0.1330 \times Ton - 0.000845 \times Toff - 0.001363 \times Gap\,Voltage - 0.000023 \times RPM - 0.000003 \times Toff \times Toff + 0.001238 \times Ton \times Toff + 0.000004 \times Toff \times Gap\,Voltage \quad \ldots (5)$$

The influence of machining parameters such as pulse on time, pulse off time, gap voltage and rotational speed on SR, MRR and WWR were analysed by generating response surfaces. The

Table 5 — The ANOVA table for fitted models.

Source	DF	Adj SS	Adj MS	F-Value	P-Value
a) For Ra					
Model	5	0.723821	0.144764	198.09	0.000
Linear	4	0.701368	0.175342	239.93	0.000
Square	1	0.022453	0.022453	30.72	0.000
Error	25	0.01827	0.000731		
Lack-of-Fit	19	0.011223	0.000591	0.5	0.882
Pure Error	6	0.007047	0.001174		
Total	30	0.742091			
S = 0.0270334; R-sq = 97.54%, R-sq(adj) = 97.05%; R-sq(pred) = 95.95%					
b) For MRR					
Model	9	59.6124	6.6236	250.35	0.000
Linear	4	57.9068	14.4767	547.17	0.000
Square	4	1.525	0.3812	14.41	0.000
2-Way Interaction	1	0.1806	0.1806	6.83	0.016
Error	21	0.5556	0.0265		
Lack-of-Fit	15	0.4712	0.0314	2.23	0.165
Pure Error	6	0.0844	0.0141		
Total	30	60.168			
c) For WWR					
Model					
Linear	7	0.001946	0.000278	931.39	0.000
	4	0.001934	0.000483	1620.08	0.000
Square	1	0.000002	0.000002	8.34	0.008
2-Way Interaction	2	0.000009	0.000005	15.54	0.000
Error	23	0.000007	0.000000		
Lack-of-Fit	17	0.000003	0.000000	0.36	0.954
Pure Error	6	0.000003	0.000001		
Total	30	0.001952			
S = 0.0005463; R-sq = 99.65%; R-sq(adj) = 99.54%; R-sq(pred) = 99.38%					

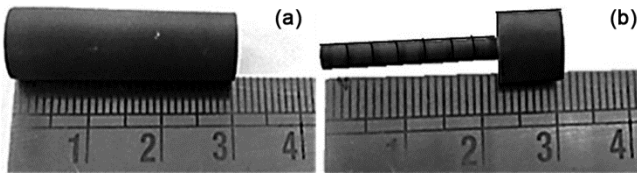

Fig. 3 — Workpiece images (a) before machining and (b) after machining.

contour plots revealed the effect of the different combination of input variables on output responses (Figure 4).

Contour plots of SR, revealed that with an increase in T_{on} value and a decrease in T_{off} value, the SR increased[33]. It was due to the increase in discharge time which resulted in a longer period of sparking which eroded the surface unevenly causing non-uniform crater formation throughout the circumferential length. It was found that SR decreased with increase in gap voltage, which was attributed due to increase in gap resistance leading to a less amount of discharge energy and lesser width of arc region[34]. With the increase in spindle speed, the roughness value decreased as the peripheral length of material passing the spark zone per unit time increased, while discharge energy available for machining remained constant[35].

MRR largely depends on discharge energy and increases with the rise in discharge energy. The increment in pulse on time and decrement in pulse off time increases the discharge energy as spark duration increases[33]. Decrease in gap voltage led to lower spark gap due to which breakdown takes place rapidly, increasing the count of discharge per unit time[36]. With lower spindle speed, higher removal rates were achieved due to reduced circumferential length of material per unit time available for removal, which led to rise in arc region and increase in the discharge energy[37].

Wire wear occurs due to the erosion of wire material by a series of sparks that takes place amid the

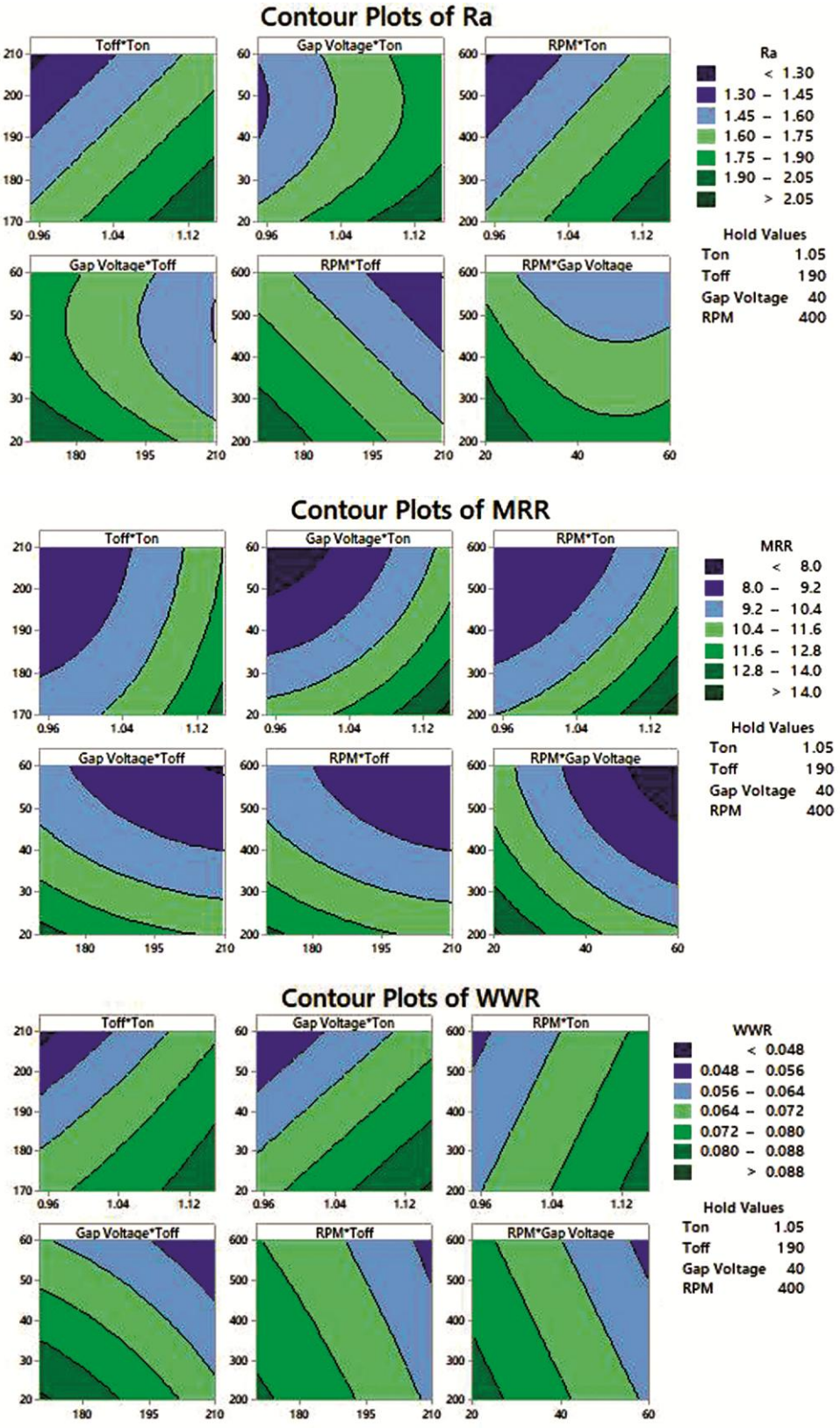

Fig. 4 — Contour plots exhibiting the effect of technological factors on (a) SR, (b) MRR and (c) WWR.

wire and the workpiece. The increase in spark energy erodes the wire and increases wire wear. The influence of technological factors on WWR is similar to that of MRR. It increased with the higher value of pulse on time and lower values of pulse off time, gap voltage and spindle speed[38, 39].

Desirability optimisation technique was applied to optimise all the output responses, in search for the level of technological parameters at which optimal value of responses can be achieved. Any combination of responses can be optimised at the same time using this approach. For the given multi-objective problem, SR and WWR were minimized, whereas MRR was maximized simultaneously. The optimal level values of input parameters for optimal responses and their combination are shown in Table 6 and optimisation plot for all the responses simultaneously is shown in Figure 5.

The confirmatory experiments were performed to validate the results obtained by desirability function optimization technique. The results of the confirmatory test are represented in Table 7. It also shows the resemblance of the predicted responses with the experimental values achieved during machining under optimal level of machining parameters.

Figure 6 shows the workpiece surface before machining. SEM images (Fig. 7) reveals the quality of the machined surfaces. The machined surface quality depends on the level of machining parameters used during machining. Machining with higher level of parameters lead to the generation of large discharge energy and detoriates the surface quality, as compared to the surface quality obtained during machining with low level of parameters[40– 42]. Surface anomalies in WEDT process were observed due to heat generated by the electrical discharge. Shallow craters and voids were observed on the machined surface (Fig. 7a) which was primarily formed because of partial melting of metal surface and again re-solidifying on the machined surface itself. Globular debris observed

Table 6 — The optimal settings of parameter for responses and their combinations.

Response	Pulse on time (µs)	Pulse off time (µs)	Gap voltage (Volt)	Rotational speed (RPM)
Ra	0.95	210	50	600
MRR	1.15	170	20	200
WRR	0.95	210	60	600
MRR, Ra & WRR	1.15	210	30	600

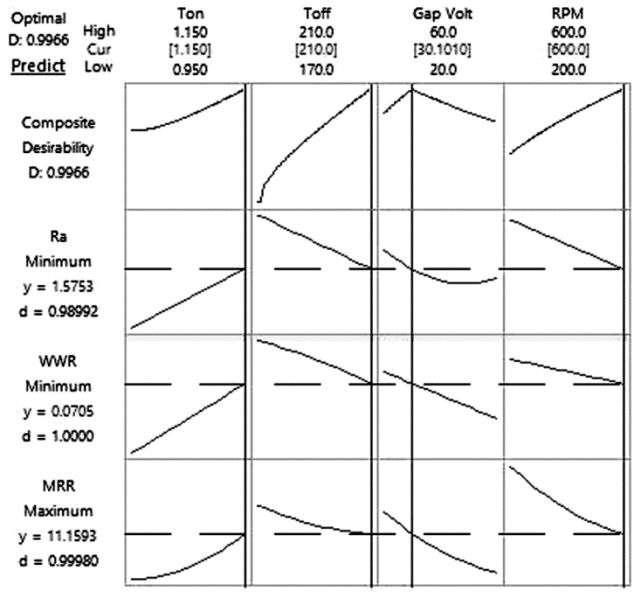

Fig. 5 — Optimisation plot for minimum SR, maximum MRR and minimum WWR.

Table 7 — Results of confirmatory test.

	Optimal condition	
	Prediction	Experiment
a) For Ra		
Level	A1B5C4D5	
Value	1.066 µm	1.131 µm
b) For MRR		
Level	A5B1C1D1	
Value	18.24 mm^3/min	17.33 mm^3/min
c) For WWR		
Level	A1B5C5D5	
Value	0.0323	0.0346
d) For Ra, MRR and WWR		
Level	A5B5C2D5	
Value	1.575 µm, 11.16 mm^3/min, 0.0705	1.654 µm, 10.49 mm^3/min, 0.0754

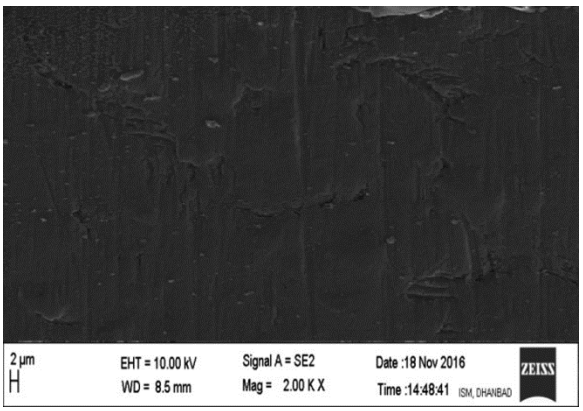

Fig. 6 — FESEM image of workpiece sample before machining.

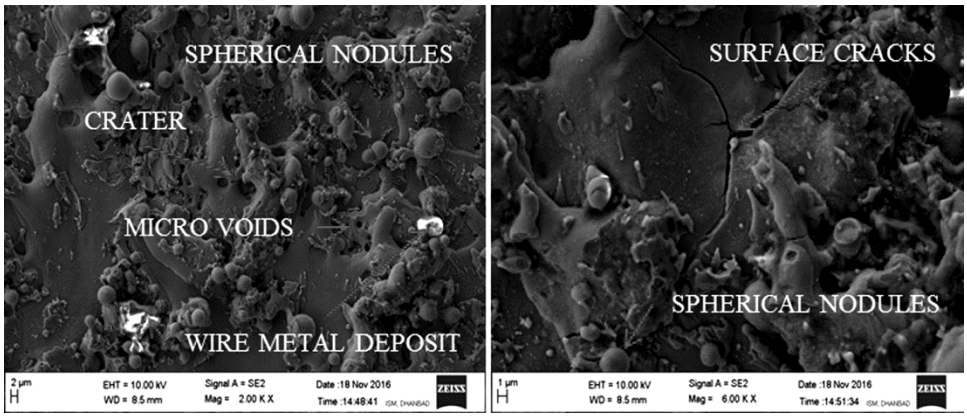

Fig. 7 — FESEM images of machined surfaces.

on the machined surface may be attributed to property of titanium alloys to easily form oxides under high temperature conditions[43]. The presence of oxides is confirmed by Energy-dispersive X-ray spectroscopy analysis of the machined surface (Fig. 8). Due to these defects were also formed due to the explosion of pressure bubble generated during machining. Non-uniform melting of the metal surface led to generation of thermal and residual stresses which were the primary reasons for the generation of cracks in the machined surface[6]. Formation of surface cracks (Fig. 7b) was also formed due to incursive carbon particle that did not wash away by the dielectric, and during cooling it contracted at a faster rate than the original material initiating a crack. Spherical nodules were formed by the action of surface tension acting upon the molten metal formed during melting of the workpiece. Some traces of deposition of wire material were also seen on the surface of the workpiece, resulted due to melting and partial improper flushing of the wire electrode.

Figure 9 (a, b) depicts the recast layer thickness deposited of the material circumference during machining of workpiece material. This layer was formed due to improper flushing of molten metal formed during melting of the material, which resulted in re-solidification of the molten metal on the workpiece surface itself[44]. The recast layer thickness of 12 - 15µm thick was observed under high MRR parameter condition which is due to high melting of the workpiece surface. Whereas, 7-9 µm thick layer of deposited metal was observed for optimal surface finish condition. This recast layer deposited on the machined surface should be avoided as it hampers the surface quality along with a decrease in mechanical property like hardness throughout the layer thickness.

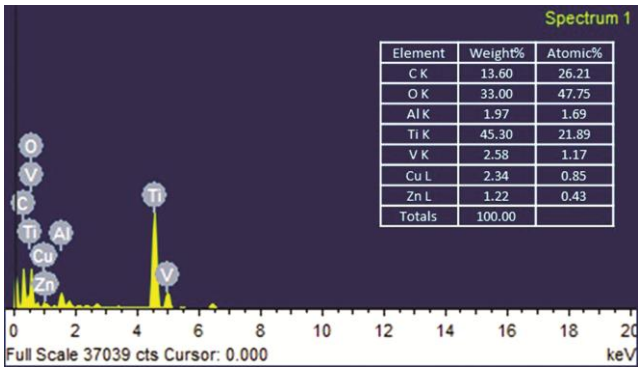

Fig. 8 — EDS analysis of the machined surface.

Figure10 (a, b) shows the wire surface morphology before and after the machining. Initially surface tearing marks were observed on the unused wire which can be due to wire drawing. During machining, due to electrical discharges, surface of the wire gets eroded and result in melting of the wire material and generation of surface cracks on the wire surface. Small craters are formed due to the effect of explosion of pressure bubble after collapsing of the spark generated. The wire metal gets eroded from the surface of the wire and deposit on the workpiece material being machined, which was observed in the SEM images of the workpiece material after machining[45, 46]. Wire material also re-solidified on its own surface due to improper flushing which in turn makes the surface rougher and detoriate the dimensional accuracy of the wire.

The dimension of the wire changed after machining due to erosion during the turning process. Figure 11 shows the change in dimension of the wire before and after machining. The change in wire dimension restricted the further use of the same wire for precise cutting. Also reusability of the wire is limited by the

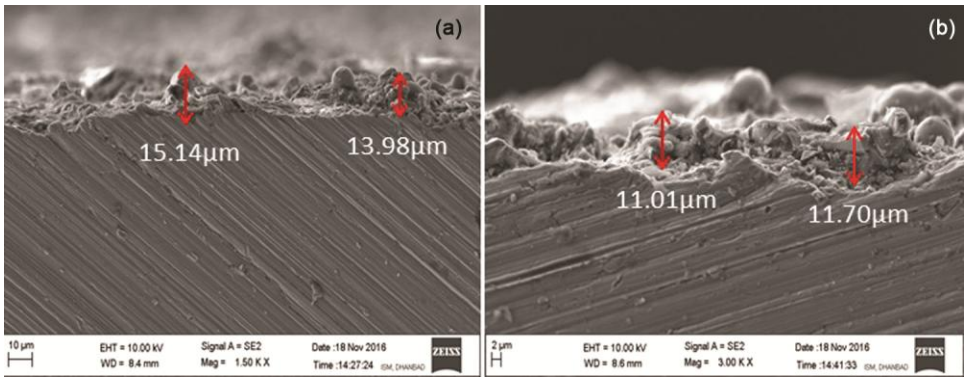

Fig. 9 — Recast layer thickness (a) for optimum MRR and(b) for optimum surface finish.

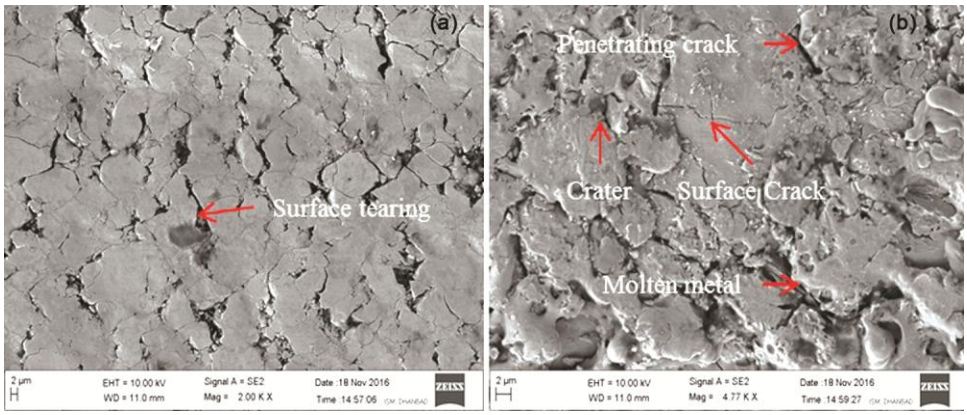

Fig. 10 — Surface morphology of wire surface (a) before machining and (b) after machining.

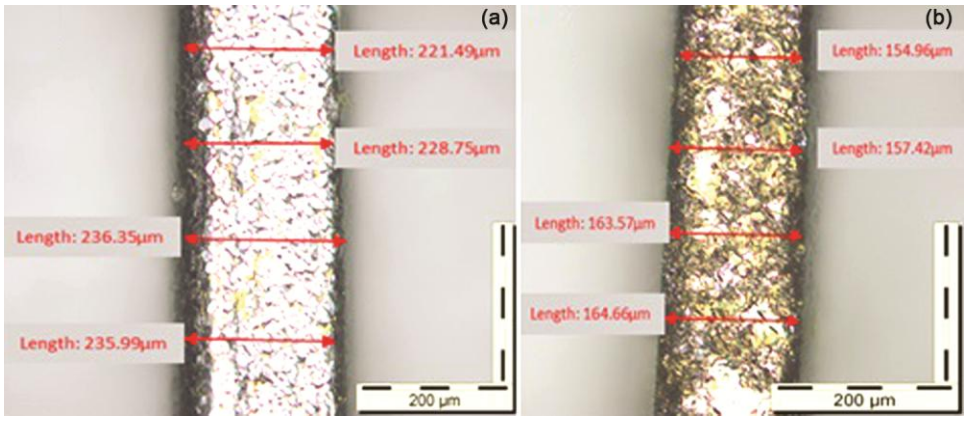

Fig. 11— Microscopic image of wire (a) before machining and (b) after machining.

final diameter of the wire obtained after each machining run. The chances of wire breakage increase significantly with the thinning of wire. The wire wear can be reduced by using the appropriate level of input parameter which would result into minimum wire wear.

4 Conclusions

The influence of process parameters on SR, MMR and WWR of Ti6Al4V cylindrical workpiece has been studied. Mathematical models for performance responses of wire electrical discharge turning were developed. On the basis of the experimental results, it can be concluded that:

(i) WEDT process can be used effectively to turn Ti6Al4Vworkpiece as a result it may eliminate the problem of rapid tool wear which occurs in conventional metal cutting.

(ii) Optimal SR of 1.131 µm, MRR of 17.33 mm^3/ min and WRR of 0.0346 was achieved while machining at optimal parametric setting obtained by desirability optimisation technique.

(iii) Surface morphology images revealed micro-cracks, micro-voids, craters and spherical nodules that took place during machining of the workpiece. Recast layer for the optimum surface finish was observed in the range of 7-9 µm whereas for optimum MRR it was nearly about 12 – 15 µm. These surface irregularities may be eliminated by existing post processing operations.

(iv) Wire surface degraded and wore out largely due to discharges occurred during machining. The dimensional change of the wire was also observed which made it unfit for reuse.

References

1 Çelik Y H & Karabiyik A, *Indian J Eng Mater Sci*, 23 (2016) 349.

2 Srivastava A K, Dixit A R & Tiwari S, *Indian J Eng Mater Sci*, 23 (2016) 171.

3 Srivastava AK, Dixit & AR Tiwari S, *Sci Eng Compos Mater*, 25(2016) 213.

4 Kunieda M, Lauwers B, Rajurkar K P & Schumacher B M, *CIRP Ann Technol*, 54 (2005) 64.

5 Chiang K T& Chang F P, *J Mater Process Technol*, 180 (2006) 96.

6 Guu Y H & Hou M T K, *Mater Sci Eng A*, 466 (2007) 61.

7 Qu J, Shih A J & Scattergood R O, *J Manuf Sci Eng*, 124 (2002) 702.

8 Luo Y F, *J Mater Process Technol*, 55 (1995)380.

9 Ramasawmy H & Blunt L, *J Mater Process Technol*, 148 (2004) 155.

10 Yan M T & Lai Y P, *Int J Mach Tools Manuf*, 47 (2007)1686.

11 Masuzawa T, Fujino M, Kobayashi K & Suzuki T, *Bull Jpn Soc Precis Eng*, 20 (1986)117.

12 Qu J, Shih A J & Scattergood R O, *J Manuf Sci Eng*, 124 (2002) 708.

13 Mohammadi A, Tehrani A F, Emanian E & Karimi D, *Int J Adv Manuf Technol*, 39 (2008) 64

14 Haddad M J & Tehrani A F, *J Mater Process Technol*, 198 (2008) 77.

15 Haddad M J, Tajik M, Tehrani A F, Mohammadi A & Hadi M, *Int J Mater Form*, 2 (2009) 167.

16 Haddad M J, Alihoseini F, Hadi M, Hadad M, Tehrani A F & Mohammadi A, *Int J Adv Manuf Technol*, 46 (2010) 1119.

17 Janardhan V & Samuel G L, *Int J Mach Tools Manuf*, 50 (2010) 775.

18 Gjeldum N, Veža I, & Bilic B, *Trans FAMENA*, 35 (2011) 27.

19 Weingärtner E, Wegener K & Kuster F, *J Mater Process Technol*, 212 (2012) 1298.

20 Weingärtner E, Wegener K & Kuster F, *Procedia CIRP*, 6 (2013) 238.

21 Dhake H G & Samuel G L, *Int J Mach Mach Mater*, 12 (2012) 252.

22 Giridharan A, Samuel G L, *Int J Manuf Technol Manag* 27 (2013) 170.

23 Garg M, Jain A & Bhushan G, *Arab J Sci Eng*, 39 (2014) 1465.

24 Zhu Y, Liang T, Gu L & Zhao W, *Procedia Manuf*, 5 (2016) 849.

25 Kanthababu M, Jegaraj J J R & Gowri S, *Int J Manuf Technol Manag*, 30(2016) 216.

26 DiBitonto D D, Eubank P T, Patel M R & Barrufet M A, *J Appl Phys*, 66 (1989) 4095.

27 Pramanik A & Littlefair G, *Mach Sci Technol*, 19 (2015) 1.

28 Sharma A, Sharma M D, Sehgal R, *Arab J Sci Eng*, 38 (2013) 3201.

29 Myers R H, Montgomery D C & Anderson-Cook CM, Response surface methodology: process and product optimization using designed experiments (John Wiley & Sons, New Jersey), 4thEdn, ISBN: 978-1-118-91601-8, (2016), p. 9.

30 Khuri A I & Mukhopadhyay S, *Comput Stats*, 2 (2010) 128.

31 Tosun N & Cogun C, *J Mater Process Technol*, 134 (2003) 273.

32 Montgomery DC, Design and analysis of experiments (John Wiley & Sons,New Jersey), 8thEdn, ISBN: 978-1-118-09793-9, (2017), p. 486.

33 Mahapatra S S & Patnaik A, *Indian J Eng Mater Sci*, 13 (2006) 494.

34 Manna A & Bhattacharyya B, *Int J Adv Manuf Technol*, 28 (2006) 67.

35 Janardhan V & Samuel G L, *Int J Mach Tools Manuf*, 50 (2010) 775.

36 Kumar M & Singh H, *Indian J Eng Mater Sci*, 23 (2016)223.

37 Srivastava A K, Nag A, Dixit A R, Hloch S, Tiwari S, Scucka J & Pachauri P, *Sci Eng Compos Mater*, 26 (2019) 122.

38 Goswami A & Kumar J, *Eng Sci Technol Int J*, 17 (2014) 173.

39 George P M, Raghunath B K, Manocha L M & Warrier A M, *J Mater Process Technol*, 145 (2004) 66.

40 Srivastava A K, Nag A, Dixit A R,Tiwari S, Scucka J, Zelenak M, Hloch S & Hlaváček P, *J Manuf Process*, 28 (2017) 11.

41 Nag A, Ščučka J, Hlavacek P, Klichová D, Srivastava A K, Hloch S, Dixit A R, Foldyna J & Zelenak M, *Int J Adv Manuf Technol*, 94 (2017) 2293.

42 Srivastava A K, Nag A, Dixit A R, Ščučka J, Hloch S, Klichová D, Hlaváček P & Tiwari S, *Measurement*, 131 (2019) 628.

43 Şimşek B, İç YT& Şimşek EH, *Arab J Sci Eng*, 41 (2016) 1435.

44 Sandomierski M, Buchwald T, Strzemiecka B, Voelkel A, *Acta - Part A Mol Biomol Spectrosc*, 191 (2018) 27.

45 Ekmekci B, *Appl Surf Sci*, 253 (2007) 9234 .

46 Pramanik A & Basak A K, *Wear*, 346 (2016)124.